Digital Object Identifier (DOI): 10.1109/ECCE.2018.8557682

2018 IEEE Energy Conversion Congress and Exposition (ECCE)

Active Thermal Control of Asynchronously-Connected Grids Considering Load Sensitivity to Voltage

Markus Andresen
Giovanni De Carne
Mike Schloh
Marco Liserre

Suggested Citation

M. Andresen, G. De Carne, M. Schloh and M. Liserre, "Active Thermal Control of Asynchronously-Connected Grids Considering Load Sensitivity to Voltage," 2018 IEEE Energy Conversion Congress and Exposition (ECCE), Portland, OR, 2018, pp. 4070-4077.

Active Thermal Control of Asynchronously-Connected Grids Considering Load Sensitivity to Voltage

Markus Andresen, Giovanni De Carne, Mike Schloh and Marco Liserre
Chair of Power Electronics, Christian-Albrechts-Universität zu Kiel, Germany
Email: ma@tf.uni-kiel.de, gdc@tf.uni-kiel.de, miks@tf.uni-kiel.de, ml@tf.uni-kiel.de

***Abstract*—A new concept in the power system management is the asynchronous connection of grids. This connection occurs at different voltage and power level: high voltage, with HVDC systems, and medium/low voltage, with back-to-back converters and Smart Transformers. The decoupling of the power flow between the two grids allows higher controllability, including the possibility to control grid voltage and frequency independently in the two grids. This work aims to investigate and mitigate the thermal stress in grid-forming converters (e.g., Smart Transformers) applying a load voltage-sensitivity control. Depending on the nature of the loads, their power consumption varies with the voltage. This response is dependent on the connected loads and can be characterized by constant power (independent from the voltage), constant current (linearly dependent on the voltage) and constant impedance behavior (squared-dependent on the voltage). The sensitivity to voltage is exploited to control the load power consumption, reducing the junction temperature fluctuations and thus the power semiconductors stress. As a consequence, the converter operational range can be increased, reducing at the same time the stress for the power semiconductors.**

I. Introduction

The power volatility introduced by renewables calls for a fast and reliable control of power grids. As a solution to improve the grid management, the asynchronous connection of grids has been proposed [1]. It allows to decouple the grids AC power flow, and thus to control the connected grids independently. It can be implemented at different voltage level and for different purposes: in HV grids, with HVDC systems, it helps to transfer power in remote points of the transmission grid, whereas, in MV and LV grids, it helps to manage the grid as a controllable resource. At this regard, technologies such as Smart Transformers (ST) or HVDC stations represent an asynchronous connection solution for the grid [2], [3]. However, operating as grid-forming converter, the power processed by the converter cannot be controlled directly, but it depends solely on the grid power demand. Thus, depending on the power injection, the power semiconductor's in the converter can suffer from high thermal stress, caused by the intermittent power fluctuations.

To reduce the thermal stress for the semiconductors, the grid forming converter can exploit its capability to control the voltage in the grid to shape the load consumption and thus to reduce the power variations in the grid forming converter [4]. The possibility to decrease the load consumption lowering the voltage has been already considered in the Conservation Voltage Regulation (CVR) approach for energy saving purposes [5]. However, the voltage set-point is controlled in open-loop and the load sensitivity to voltage are not taken into account. Depending on the overall grid sensitivity to voltage, a decrease of the grid voltage can even increase the thermal stress for power semiconductors in the grid forming converter, that depends mainly on the grid current. In presence of constant power loads, a voltage reduction leads to a current increase, and thus to higher thermal stress. Consequently, the load sensitivity must be known before to apply the control action for a proper grid management [4], [6].

This work investigates the potential of controlling the grid voltage for increasing the maximum operating range of the grid-forming converter and for reducing the stress of the power semiconductors. The damage reduction is quantified and the obtained results are compared to the application of CVR, where the load sensitivity to voltage is not considered.

First, this work provides the basic concepts of the grid voltage sensitivity along with the importance of the junction temperature for the reliability of the power converter. Section III demonstrates the capability of the voltage and frequency to the stress in case of a constant impedance, constant power and constant current load. In the fourth section, experimental results are shown to validate the potential of the introduced approach and the results are concluded in section V.

II. Grid voltage sensitivity and junction temperature modeling

This section first introduces the concepts of different load behaviors resulting in different sensitivity to the grid voltage. The second subsection examines on the importance of the power semiconductor's junction temperature and provides the fundamentals for junction temperature modeling.

A. Load behavior and grid voltage sensitivity

Grid connected loads can be characterized by a certain power level, certain dynamic behavior and a certain behavior with respect to grid voltage variations. Thereby, the grid voltage is the only parameter, which can be affected by control of the grid feeding converter. The behavior of the loads with respect to grid voltage variations can be described with three characteristic behaviors:

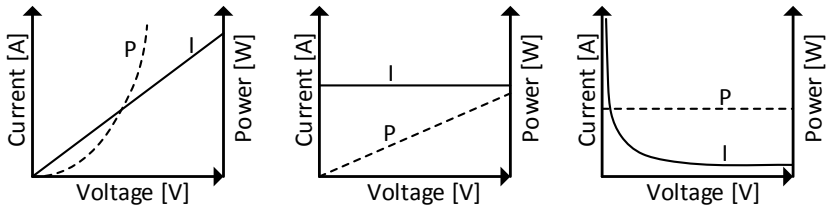

Fig. 1: Current and Power characteristics for constant impedance load (left), constant current load (centre) and constant power load (right).

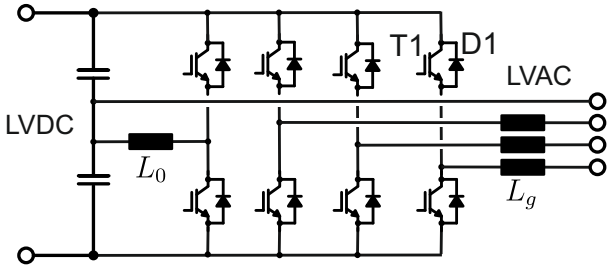

Fig. 2: Two level voltage source converter.

- Constant impedance load (e.g. incandescent lighting, unregulated motors)
- Constant power load (e.g. converter feed variable speed drives, computer, TV)
- Constant current load (e.g. fluorescent lighting)

The characteristic behavior of the different load types is visualized in Fig. 1. In addition to the power consumption of the load, the current is sketched in dependence of the grid voltage, because the current is primary responsible for the losses in power semiconductors. This is shown for the constant impedance case in (1)

$$P = \frac{V^2}{R} = P_0 \cdot \left(\frac{V}{V_0}\right)^2 \quad \text{for constant impedance loads} \quad (1)$$

where P is the power demand at the voltage V and P_0 is the reference power demand at reference voltage V_0. R is the resistance of the load. The constant current load and the constant power load are expressed with the current I in (2) and (3), respectively:

$$P = V \cdot I = P_0 \cdot \left(\frac{V}{V_0}\right)^1 \quad \text{for constant current loads} \quad (2)$$

$$P = P_0 = P_0 \cdot \left(\frac{V}{V_0}\right)^0 \quad \text{for constant power loads} \quad (3)$$

As it can be interpreted from Fig. 1 and (1)-(3), a variation of the voltage affects different responses of the load current for the different load types. In particular for the constant impedance load case, an increase of the grid voltage has an opposite effect than for the constant power load. For this reason, knowledge about the load types is of high importance, if the grid voltage is changed. Moreover, if the goal is a reduction of the power semiconductor's stress, the behavior of the loads needs to be known.

A common way to characterize the load composition of a grid is the use of ZIP indicators K_Z, K_I, and K_P, representing the constant impedance load, constant current load and constant power load share, respectively. $K_Z = 0.5$ means that 50% of the load are constant impedance loads. The sum of the three factors equals one as expressed with (4) [7]:

$$K_Z + K_I + K_P = 1 \quad (4)$$

Based on this definition, the power consumption of the load P_{load} in a grid can be described in dependence of the base power P_0 at the reference voltage V_0 and the grid voltage V:

$$P_{load}(V) = P_0 \cdot \left(K_Z \cdot \left(\frac{V}{V_0}\right)^2 + K_I \cdot \frac{V}{V_0} + K_P\right) \quad (5)$$

If generation in the grid is considered, the power of the grid feeding converter can either be injected into the grid or the power flow can reverse. Moreover, the generators will act as constant power sources independently from the grid voltage. As a result for non-reversing power flow, the power, which needs to be processed by the grid forming converter can be described with (6) [4].

$$P(V) = P_0 \cdot \left(\frac{V}{V_0}\right)^{K_L \cdot \frac{P_{load}}{P_{load} - P_{gen}}} \quad (6)$$

It can be interpreted from the equation, that the generation in the grid affects a higher sensitivity of the load current to the grid voltage in case of the presence of constant impedance and constant current loads.

B. Thermal stress and junction temperature modeling

The wear out and failure mechanisms of power semiconductors are caused by thermal stress, which affects the interfaces between layers of materials with different coefficients of thermal excursion. During operation, the mission profile is causing power variations, which are affecting variations of losses and therfore junction temperature variations. These variations cause the wear-out and potentially result in a failure of the devices. The most commonly found failure mechanisms are bond wire liftoff and solder fatigue [8].

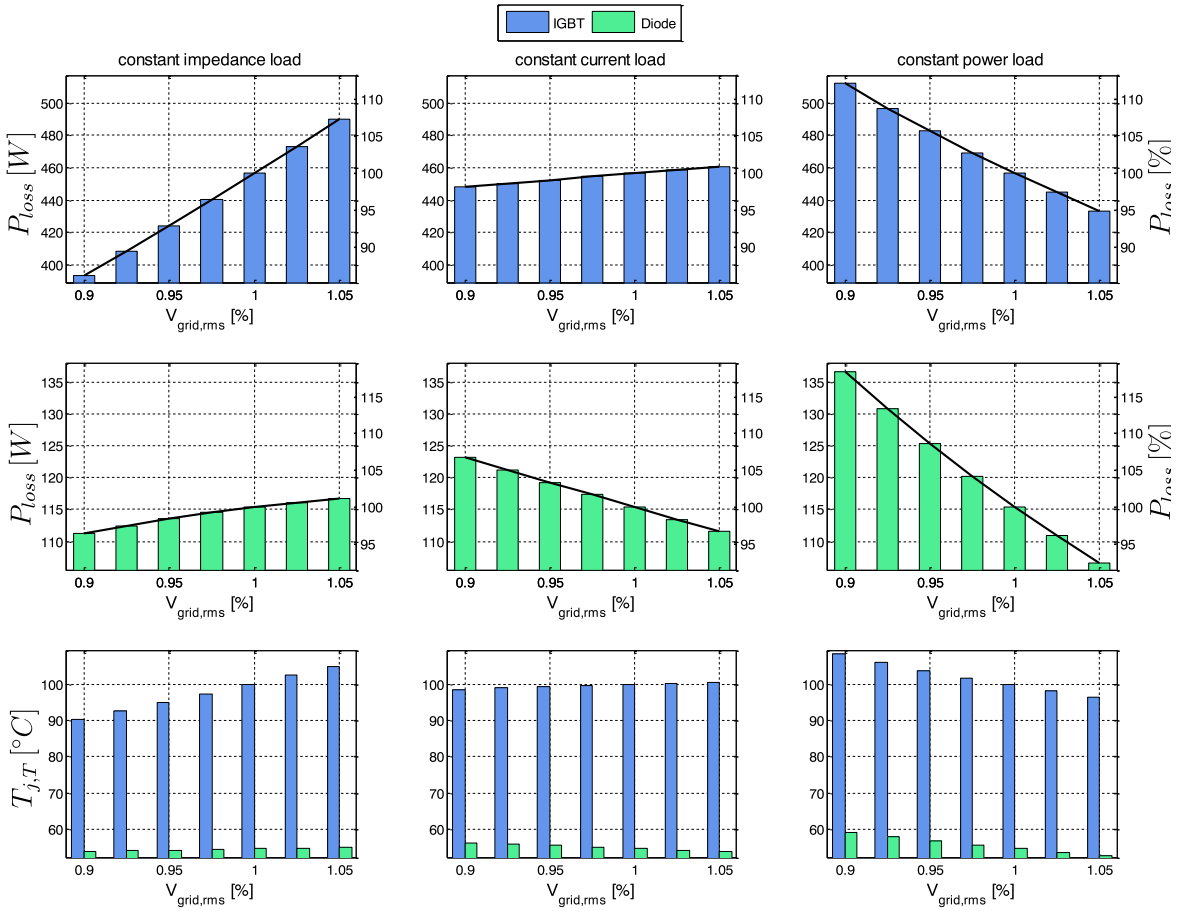

Fig. 3: Power losses and junction temperature of IGBT and diode for varying grid voltage $V_{\text{grid,rms}}$ and different load types. No distributed generation.

A common way to express the lifetime of a power semiconductor is schematically expressed in (7), where the lifetime of semiconductors is quantified by the manufacturer in dependence of the number of junction temperature swings N_f with the magnitude ΔT_j and the average junction temperature $T_{j,av}$ with the fitting parameters a_1,a_2 and a_3. Remarkably, the magnitude of the junction temperature has exponential influence on the lifetime of the devices.

$$N_f = a_1 \cdot (\Delta T_j)^{a_2} e^{\frac{a_3}{T_{j,av}}} \tag{7}$$

For the evaluation of the lifetime, the damage is commonly accumulated linearly with Miner's rule shown in (8)

$$C = \sum_i \frac{n_i}{N_i} \tag{8}$$

Here C is the cumulative damage, n_i the number of cycles in the stress range i and N_i the number of cycles to failure in the $i-th$ stress range. Thus, the more thermal cycles occur in the mission profiles the more the cumulative damage will rise. If the cumulative damage reaches 1, the module will fail according to the model [9].

As a consequence, it is targeted to reduce junction temperature fluctuations for increasing the lifetime of the power semiconductors. The reduction of the junction temperature fluctuations by means of software is referring to active thermal control [10] and in the following, it is applied by controlling the grid voltage.

III. Impact of Grid Voltage Variation on Junction Temperature

In this section, it is investigated how the grid voltage control can be used to reduce thermal stress for the power semiconductors in a power converter. Therefore, the losses of the different load types are derived in dependence of the grid voltage for a two level voltage source converter as shown in Fig. 2. Based on these losses the junction temperature is derived. Therefore, the switching losses and the conduction losses of the power semiconductors need to be derived. These losses can be split into conduction and switching losses for the switches and diodes . For the switches, IGBTs are considered and the switching losses $P_{sw,T}$ and the conduction losses $P_{cond,T}$ can be derived with (9) and (10) respectively [11].

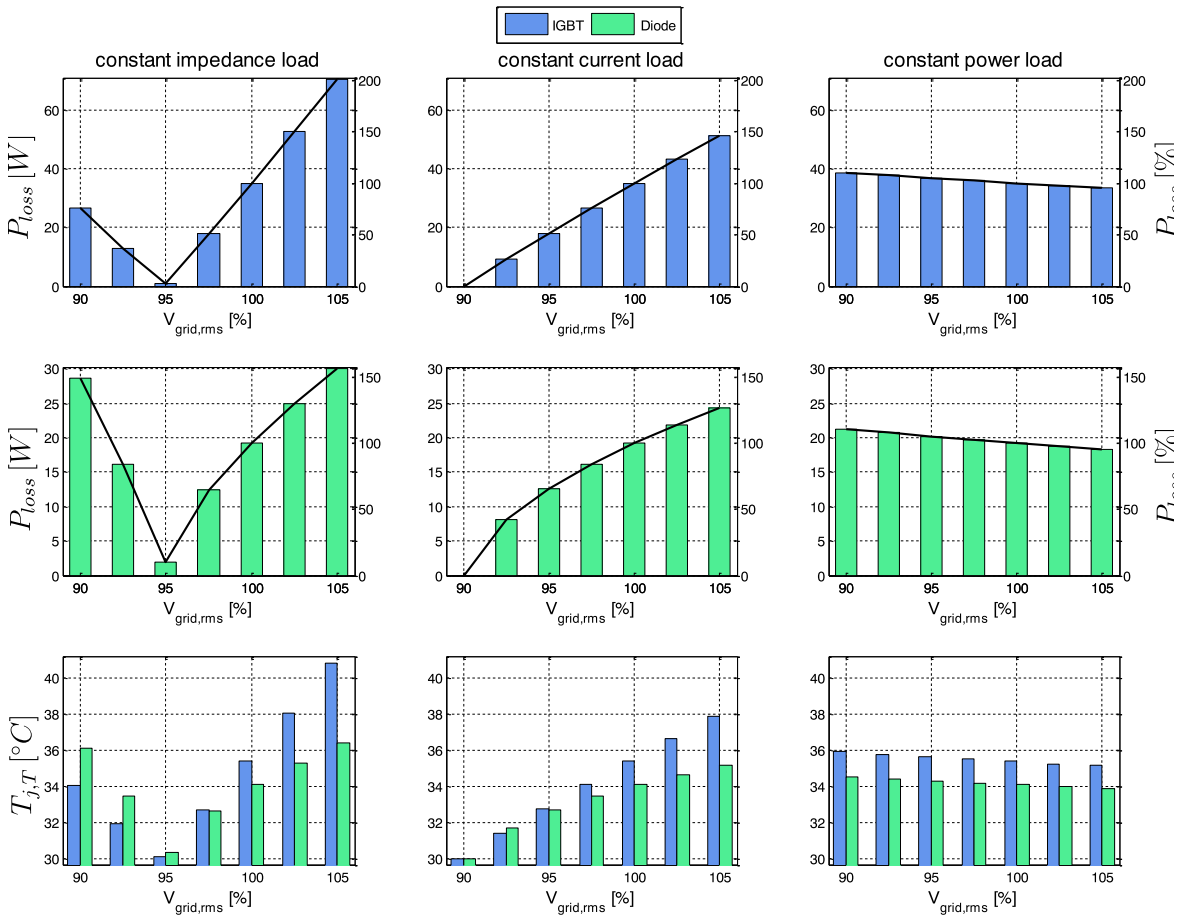

Fig. 4: Power losses and junction temperature of IGBT and diode for varying grid voltage $V_{grid,rms}$ and different load types. 90% distributed generation.

$$P_{sw,T} = f_{sw} \cdot E_{sw} \frac{\sqrt{2}}{\pi} \cdot \frac{I}{I_{ref}} \cdot (\frac{V}{V_{ref}})^{1.3} (1 + C_{sw}(T_j - T_{ref})) \quad (9)$$

$$P_{cond,T} = (\frac{1}{2\pi} + \frac{m \cdot \cos\varphi}{8}) v_{ce,0}(T_j) \cdot I + (\frac{1}{8} + \frac{m \cdot \cos\varphi}{3\pi}) r_{ce}(T_j) \cdot I^2 \quad (10)$$

In this equation f_{sw} is the switching frequency, m the modulation index, $cos(\varphi)$ the power factor, C_{sw} is a parameter showing the temperature dependence of the losses and E_{sw} is the sum of the turn-on and turn-off losses at the reference current I_{ref}, the reference voltage V_{ref} and the reference temperature T_{ref}. The conduction losses are approximated with the temperature dependent voltage drop $v_{ce,0}$ and the resistance r_{ce}. In a similar way, the conduction losses of the diodes $P_{cond,D}$ and the reverse recovery losses P_{rr} can be expressed with (11) and (12), respectively.

$$P_{rr} = f_{sw} \cdot E_{rr} \frac{\sqrt{2}}{\pi} \cdot \frac{I}{I_{ref}} \cdot (\frac{V}{V_{ref}})^{1.3} (1 + C_{SW}(T_j - T_{ref})) \quad (11)$$

$$P_{cond,T} = (\frac{1}{2\pi} + \frac{m \cdot \cos\varphi}{8}) v_{d,0}(T_j) \cdot I + (\frac{1}{8} + \frac{m \cdot \cos\varphi}{3\pi}) r_d(T_j) \cdot I^2 \quad (12)$$

In these equations, E_{rr} represents the reverse recovery losses, $v_{d,0}$ is the on state voltage drop of the diode and r_d is the resistance of the diode. For obtaining the junction temperature in stationary conditions $T_{j,T}$, the losses of the transistors can be multiplied with the thermal resistance between junction and case $R_{th,jc}$ and need to be added to the case temperature T_c. This is shown for the junction temperature of the IGBT in (13), where the conduction and switching losses of the IGBT are considered.

$$T_{j,T} = T_c + R_{th,jc} \cdot (P_{cond,T} + P_{sw,T}) \quad (13)$$

This equation only holds for stationary analysis. However, it is used in the following to evaluate the potential of the grid voltage variation for the thermal stress reduction of the semiconductors. Fig. 3 demonstrates the effect of varying the grid voltage between $V_{grid,rms} = 0.9...1.05\,pu$ for the three different load types without additional distributed generation in the grid. As expected, it can be seen that the losses can be

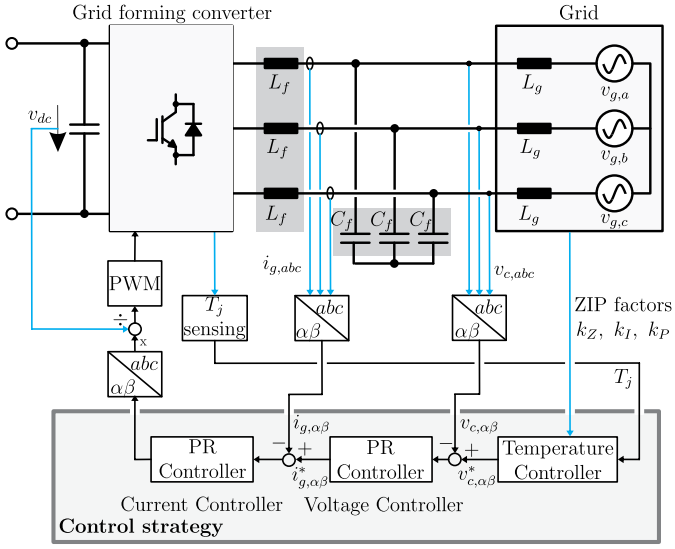

Fig. 5: Scheme of the proposed grid forming control.

influenced and therefore the junction temperature. The highest potential exists for the constant impedance load, whereas the constant current load has the lowest potential.

Fig. 4 considers distributed generation in the grid, which increases the capability to control the losses and therefore the junction temperature significantly. Here, the normed losses can be varied in a much higher range, even if the overall losses are lower than in the case before. With respect to the sizing of the converter, this offers the potential to reduce the size of the grid forming converter, while still fulfilling the required operations. However, in this section, the grid voltage control is utilized to reduce the thermal stress for the power semiconductors.

IV. Reduction of the Junction Temperature Fluctuations

In this section the thermal controller design is demonstrated and an evaluation of the junction temperature for the most extreme load cases is shown.

A. Temperature controller design

For the goal of the thermal stress reduction, the junction temperature is proposed to be controlled by controlling the grid voltage. This is done in an additional cascaded loop as shown in Fig. 5. The junction temperatures of the power semiconductors is sensed as well as the load sensitivity for setting the reference voltage of the grid. With this information, the grid voltage is controlled with two cascaded PR controllers.

The temperature controller is implemented with a PI-controller and the open loop transfer function of the system $G_{th,ol}(s)$ is expressed with:

$$G_{th,ol}(s) = \frac{T_{j,T(s)}}{V(s)} = G_V(s) \cdot G_{th}(s) \cdot G_{loss}(s) \cdot G_{PI}(s) \qquad (14)$$

In this equation, $G_V(s)$ is the closed loop voltage controller, $G_{th}(s) = Z_{th,jc}(s)$ is the thermal impedance of the power module, G_{loss} is the transfer function between losses and grid voltage and $G_{PI}(s)$ is the transfer function of the PI-controller. As it can be seen in (9) and (10), the transfer function between the grid voltage and the power semiconductor losses is partially independent from the voltage and partially non-linear. However, due to the small variation of the grid voltage, it is approximated with $G_{loss} = k_{loss}$. This results in the challenge of small time constants related to the thermal impedance and the resultant time constant o the the voltage controller, whereas the approximated voltage controller already limits the potential dynamics of the temperature controller.

If only a single thermal chain is considered for G_{th} in (14), the open loop transfer function can be derived. Therefore, the PI-controller is tuned with the modulus optimum, resulting in the cancellation of the zero of the PI-controller with the pole of the thermal impedance. This results in:

$$G_{th,ol}(s) = \frac{K_{PI} \cdot R_{th,eq} \cdot k_{loss}}{T_i s + T_i T_d s^2} \qquad (15)$$

with the equivalent thermal resistance of the first order thermal chain $R_{th,eq}$, the time constant of the integrator T_i, the proportional gain of the integrator K_{PI} and the equivalent time constant of the voltage control loop T_d. As a result, the closed loop can be expressed with:

$$G_{th,cl}(s) = \frac{1}{1 + \frac{T_i}{K_{PI} \cdot R_{th,eq} \cdot k_{loss}} s + \frac{T_i T_d}{K_{PI} \cdot R_{th,eq} \cdot k_{loss}} s^2} \qquad (16)$$

This equation needs to be evaluated carefully, because the thermal model is only evaluated for a single thermal chain. It results in the negligence of the fast thermal dynamics (at the junction) and the slow thermal dynamics (of the cooling system). Consequently, the parameters of the PI-controller may need to be adjusted to obtain the required dynamic performance.

B. Evaluation of the impact of grid voltage control on the thermal stress

For evaluating the performance of the thermal controller, a mission profile for a grid with fast changing power cycles is considered. The profile length is chosen to be one minute in order to obtain a time period in which reasonable fast power variations occur, which can still be simulated. The applied thermal model is described in [12] and it is suitable for enabling thermal simulations with relatively long time periods of several minutes. The considered mission profile is simulated for the two most extreme load behaviors with respect to the grid voltage sensitivity, which are the constant impedance load and the constant power load. Any other mix of the load composition will have a lower grid voltage sensitivity. For the investigation of the junction temperature sensitivity to the load composition, the junction temperature is simulated for the case with constant nominal grid voltage, the application of CVS ($95\%V_0$) and the temperature control. The thermal profiles for the case of a constant impedance load are shown in Fig. 6.

In the figure, only a moving average of the junction temperature $T_{j,mean}$ is shown, because otherwise the junction

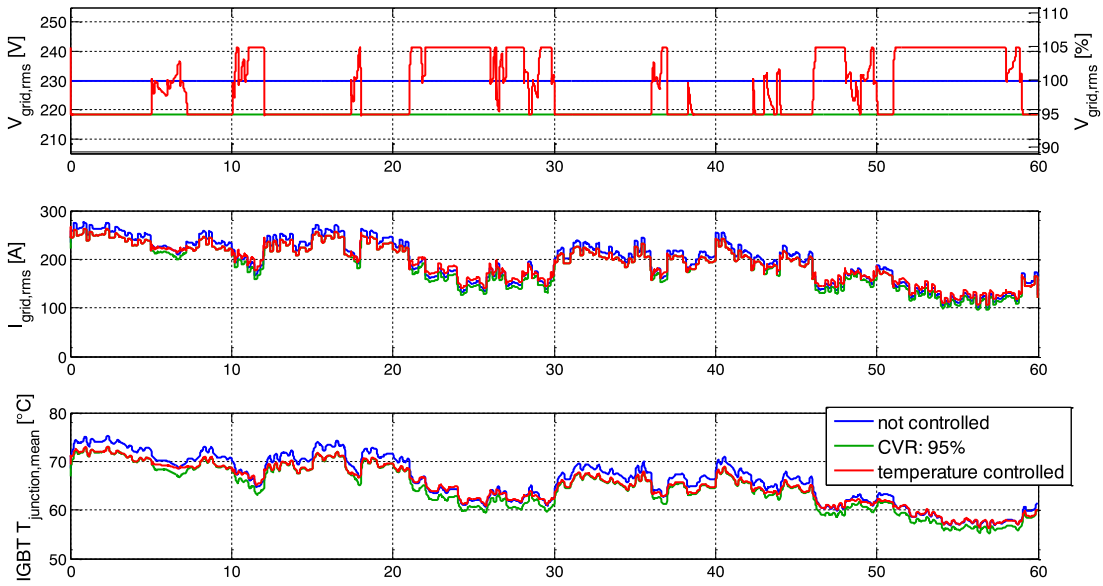

Fig. 6: Simulated junction temperature of an IGBT in the 2 level voltage source converter feeding a constant impedance load based grid for a mission profile with fast changes in the power consumption and generation. Comparison between operation with constant voltage, CVR (grid voltage = 95% of nominal grid voltage) and junction temperature control.

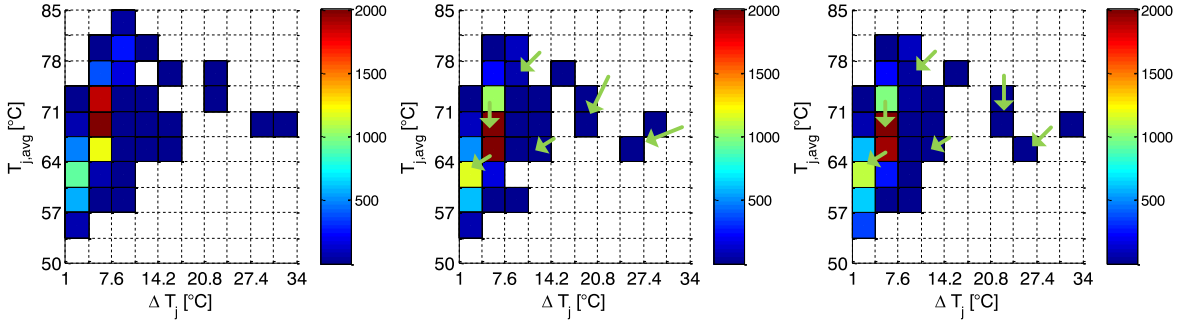

(a) (b) (c)

Fig. 7: Rainflow counted thermal cycles of the voltage control strategies of the grid feeding converter feeding a constant impedance load as shown in Fig. 6: (a) Constant nominal grid voltage, (b) CVR, and (c) temperature control.

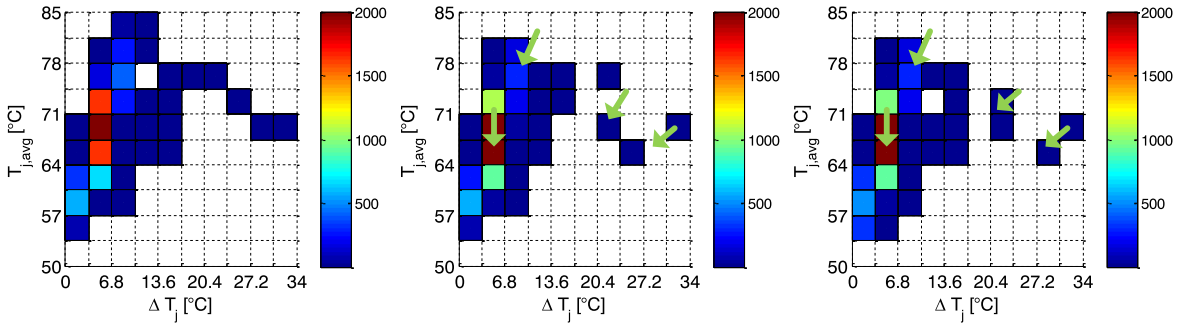

(a) (b) (c)

Fig. 8: Rainflow counted thermal cycles of the voltage control strategies of the grid feeding converter feeding a constant impedance load: (a) Constant nominal grid voltage, (b) CVR, and (c) temperature control.

temperature cycles affected by the fundamental frequency of the grid ($f_g = 50Hz$) are visually dominant. As it can be seen in the figure, the junction temperature follows the current profile, as expected. The CVS achieves a reduction of the

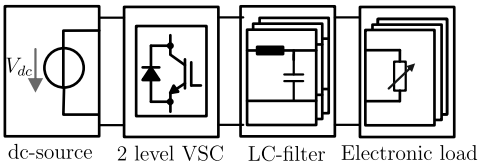

Fig. 9: Scheme of the test bench used to obtain the experimental results.

	Normalized damage	Damage reduction (CVR)	Damage reduction (temperature control)
Const. Z-load	1	40.4 %	42.7 %
Const. P-load	1	31.3 %	33.1 %

TABLE I: Reduction of the accumulate damage for the constant impedance load (Const. Z-load) and the constant power load (Const. P-load) for the simulations with constant grid voltage, application of CVS and temperature control.

load current and therefore of the temperature. The temperature control instead is acting like CVR for roughly half of the time and increases the voltage to increase the temperature during down swings of the load power demand of the grid. The related junction temperature is lower than the one of the constant voltage case and higher than the one of the CVR case.

For the evaluation of the thermal stress, Rainflow counting is applied to count the thermal cycles of the temperature profile. This is shown for the junction temperature profile of the constant impedance load under the application of the three control strategies in Fig. 7. As it can be seen, the thermal cycles are shifted to lower temperature magnitudes $T_{j,avg}$ and to lower thermal swings ΔT_j. Remarkably, the influence of the CVR and the temperature control is comparable.

The same mission profile is run for a constant power load. In this case, the results of the Rainflow counting for the junction temperature profile of the IGBT is shown in Fig. 8. Similar to the constant impedance load, the CVR and the temperature control achieve a very similar shift of the mean temperature $T_{j,avg}$ of the thermal cycles and their magnitude T.

For the evaluation of the lifetime impact of the proposed method, Miner's rule (8) is applied for the constant impedance load case and the constant power load case in with the CVR and the junction temperature control strategy. The results of the damage evaluation is normalized and shown in Table I. As it can be seen, the thermal stress reduction by applying the CVR is 40 % in case of a constant impedance load and 31 % for a constant power load, respectively. The difference compared to the active temperature control achieves in both cases an additional damage reduction of 2 %. This value is only slightly better and alone it is not sufficient to motivate the application of temperature control. However, more energy is supplied to the loads for the temperature control in case the load is not a pure constant power load. In addition the losses and thereby the thermal stress for the devices in the ST can be controlled as shown in Fig. 3 and Fig. 4.

Symbol	Description	Value
V_0 (rms)	Grid voltage (rms)	$120V$
f_g (rms)	Grid frequency	$50Hz$
L_g	Filter inductance	$3.5mH$
V_{DC}	DC-link voltage reference	$400V$
P_{load}	Load power	$5kW$
P_{gen}	Power of distributed generation	$0kW$
$[k_Z;k_I;k_P]$	ZIP composition	$[1;0;0]$

TABLE II: Parameters of the experimental setup.

V. Experimental validation

To validate the effectiveness of the proposed method, the experimental setup represented in Fig. 9 is used with the parameters shown in Table II. The junction temperature is directly measured with an Opsens Prosens system, enabling sensor response times of $5ms$. Similar to the simulation study, three cases are shown in Fig. 10. The first case shows the junction temperature undergoing a profile with constant nominal voltage, the second case shows the junction temperature for the application of CVR and the third case applies direct junction temperature control.

The results of the laboratory experiment in terms of accumulated damage are also similar to the simulation results. Rainflow counting is applied for the laboratory results, which is shown in Fig. 11. The accumulated damage reduction of the temperature control is 42.2 %, whereas the result of CVR is 34.8 % and therefore slightly lower. However, the experimental results match with the results obtained in the simulations.

VI. Conclusion

High power injection volatility increases the thermal stress in grid-forming converters, such as the LV converter in STs. Lowering the voltage to decrease the power consumption, with a mechanism, similar to CVR, may increase the thermal stress instead of decreasing it. In order to maximize the operation range of a system and for a reduction of the power semiconductor's thermal stress, the control of grid voltage considering the load sensitivity evaluation is proposed. A controller is designed, which controls the junction temperature and adapts the output voltage to reduce power fluctuations of the grid forming controller and thus the thermal stress for its power semiconductors. The results of the proposed approach are compared to the application of CVR, which does not take into account the loads sensitivity. A damage reduction for a load profile is demonstrated to be 34.8% for the CVR algorithm and 42.2% for the direct junction temperature control, making the algorithm a promising solution without causing additional costs.

Acknowledgment

This work was supported in part by the European Union/Interreg V-A Germany-Denmark, under PE: Region Project and in part by the European Research Council under the European Union's Seventh Framework Programme (FP/2007-2013)/ERC Grant Agreement no. 616344 - HEART.

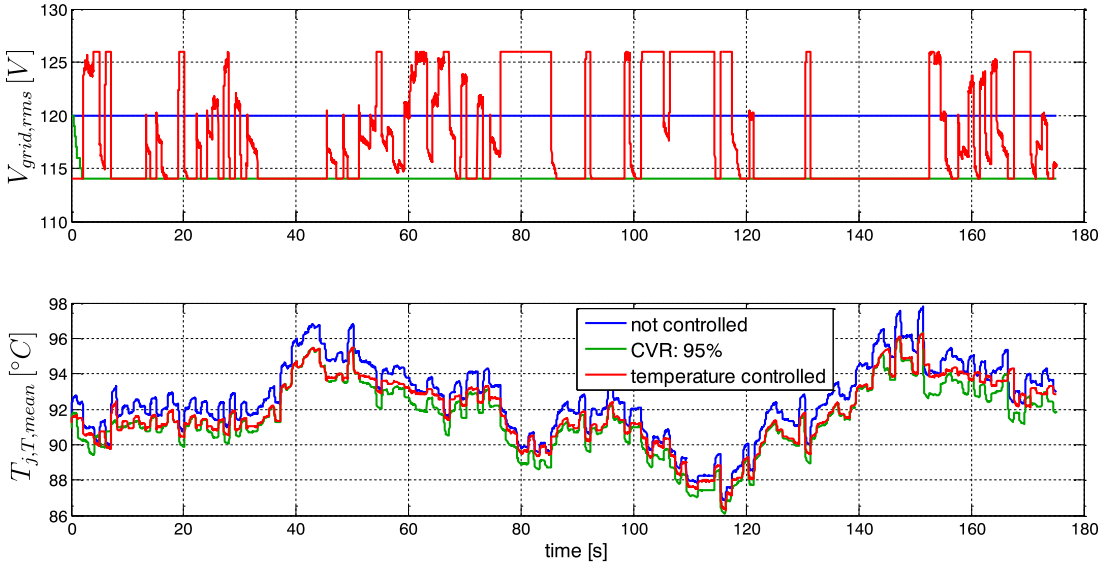

Fig. 10: Measured junction temperature of an IGBT in the 2 level voltage source converter feeding a constant impedance load based grid for a mission profile with fast changes in the power consumption and generation. Comparison between operation with constant voltage, CVR (grid voltage = 95 % of nominal grid voltage) and junction temperature control.

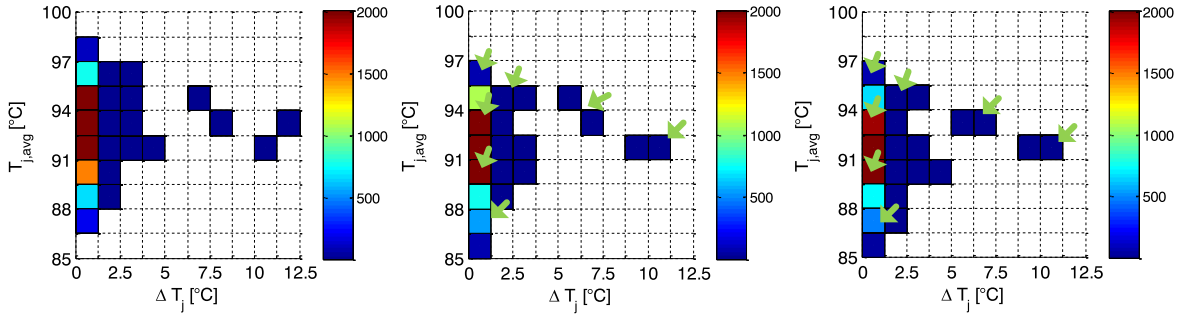

(a) (b) (c)

Fig. 11: Experimental measurement of the Rainflow counted thermal cycles in a grid forming converter feeding a constant impedance based grid as shown in Fig. 10: (a) Constant nominal grid voltage, (b) CVR, and (c) temperature control.

REFERENCES

[1] R. Abe, H. Taoka, and D. McQuilkin, "Digital grid: Communicative electrical grids of the future," *IEEE Transactions on Smart Grid*, vol. 2, no. 2, pp. 399–410, June 2011.

[2] M. Liserre, G. Buticchi, M. Andresen, G. D. Carne, L. Costa, and Z. Zou, "The smart transformer. impact on the electric grid and technology challenges," *IEEE Transactions on Industrial Electronics Magazine*, June 2016.

[3] M. Guan and Z. Xu, "Modeling and control of a modular multilevel converter-based hvdc system under unbalanced grid conditions," *IEEE Transactions on Power Electronics*, vol. 27, no. 12, pp. 4858–4867, Dec 2012.

[4] G. D. Carne, G. Buticchi, M. Liserre, and C. Vournas, "Load control using sensitivity identification by means of smart transformer," *IEEE Transactions on Smart Grid*, vol. PP, no. 99, pp. 1–1, 2017.

[5] W. Ellens, A. Berry, and S. West, "A quantification of the energy savings by conservation voltage reduction," in *2012 IEEE International Conference on Power System Technology (POWERCON)*, Oct 2012, pp. 1–6.

[6] G. D. Carne, M. Liserre, and C. Vournas, "On-line load sensitivity identification in lv distribution grids," *IEEE Transactions on Power Systems*, vol. 32, no. 2, pp. 1570–1571, March 2017.

[7] A. Bokhari, A. Alkan, R. Dogan, M. Diaz-Aguiló, F. de León, D. Czarkowski, Z. Zabar, L. Birenbaum, A. Noel, and R. E. Uosef, "Experimental determination of the zip coefficients for modern residential, commercial, and industrial loads," *IEEE Transactions on Power Delivery*, vol. 29, no. 3, pp. 1372–1381, June 2014.

[8] M. Ciappa, "Selected failure mechanisms of modern power modules," *Microelectronics reliability*, vol. 42, no. 4, pp. 653–667, 2002.

[9] H. Lu, T. Tilford, and D. Newcombe, "Lifetime prediction for power electronics module substrate mount-down solder interconnect," in *Proc. of International Symposium on High Density packaging and Microsystem Integration, HDP'07*. IEEE, 2007, pp. 1–10.

[10] M. Andresen, K. Ma, G. Buticchi, J. Falck, F. Blaabjerg, and M. Liserre, "Junction temperature control for more reliable power electronics," *IEEE Transactions on Power Electronics*, vol. 33, no. 1, pp. 765–776, Jan 2018.

[11] A. Wintrich, U. Nicolai, T. Reimann, and W. Tursky, "Application manual power semiconductors." ISLE, 2011.

[12] M. Andresen, K. Ma, G. D. Carne, G. Buticchi, F. Blaabjerg, and M. Liserre, "Thermal stress analysis of medium-voltage converters for smart transformers," *IEEE Transactions on Power Electronics*, vol. 32, no. 6, pp. 4753–4765, June 2017.